INTERNATIONAL JOURNAL OF APPLIED METHODS IN ELECTRONICS AND COMPUTERS

www.ijamec.org

International Open Access

Volume 11
Issue 03

September, 2023

Research Article

A Non-Contact Object Delivery System Using Leader-Follower Formation Control for Multi-Robots

Halil İbrahim Dokuyucu [a,*], ***Nurhan Gürsel Özmen*** [b]

[a]*General Directorate of Trabzon Water and Sewerage, Sanayi Mah. Devlet Karayolu Cad. Yaren Sok. No:1, Trabzon 61030, Türkiye*
[b]*Karadeniz Technical University, Department of Mechanical Engineering 61080, Trabzon, Türkiye*

ARTICLE INFO

Article history:
Received 21 February 2023
Accepted 30 May 2023

Keywords:
Leader-follower formation control,
Non-contact systems,
Object delivery,
Vision-based navigation

ABSTRACT

Rapid improvements in the area of multi-robot control algorithms pave the way to design and implement robotic swarms to deal with sophisticated tasks including intelligent object transportation systems. It is crucial to manage the structure of the numerous robots to behave like a whole body for task accomplishment. The leader-follower formation control approach offers a simple and reliable way of keeping the swarm formation in appropriate limits to cope with challenging tasks. Autonomous object transportation with multi-robot systems enjoy the benefits of the leader-follower formation control approach. However, most of the developed transportation systems achieve the task by locating the load onto the robots or by pushing the load in the means of a physical contact. These approaches may lead to a hardware or payload damage due to heavy loads or physical contacts respectively. In this study, a novel non-contact object delivery system is introduced for eliminating the drawbacks of physical contact between the robots and the payload. Permanent magnets are used for propulsion of the payload located on a cart with passive casters. The stability of the proposed multi-robot system is satisfied by a formation controller using potential functions method augmented with a cornering action sub-controller. The simulation results verify the effectiveness of the proposed system during a straight motion and cornering with the root mean square values of the distance between the robots as 1.46×10^{-4} [m] and 0.065 [m] respectively.

1. Introduction

Autonomous robots have become popular in the last decades since they improve the success rate of operations executed in the industry. Building up multi-robot autonomous systems can even upgrade the performance in the sense of cooperative task deployments including surveillance [1], search and delivery [2], agriculture [3], and space missions [4], [5]. When working with cooperative robotic systems, specifically in the object transportation area, three types of control strategy: 1) Formation Control, 2) Coordinated Impedance Control, and 3) Task Sequencing are observed [6]. In multi-robot systems, the formation control became one of the prominent research area that has been searched by several researchers. The formation control is defined as the movement of the multi-robot team while controlling the relative position and orientation of team members. In the literature, leader–follower based, behavior based, and virtual structure based movement strategies have been searched [7]. Moreover, the control structure of multi-robot systems can be built-up by considering three general approaches including centralized, distributed, and layered approaches [8].

In the leader-follower formation control, the main trajectory is followed by the robot assigned as the leader, whereas the follower robots try to keep specified position distances with respect to the leader [9], [10]. Different formation patterns including lattice, line, circle, and V-shape can be formed by the team members. The lattice formation can be a good solution for specific object transportation tasks [11] and field search tasks [12], whereas the line formation offers the capability of passing from narrow corridors [9]. It is important for the follower robots to estimate the leader

* Corresponding author. E-mail address: halilibrahimdokuyucu@gmail.com
DOI: 10.58190/ijamec.2023.40

robot's states to reach the convergence of formation errors to zero as introduced in [13]. A fault tolerant multi-vehicle leader-follower consensus is developed in [14], by proposing a novel fault model for a cooperative robotic uncertain system that is networked wireless. An autonomous docking capability of follower robots to increase the environmental adaptation is proposed in [15]. As the number of the agents increases in the system, the communication network becomes more important for the sake of a robust operation, where a novel event-triggered formation control strategy is proposed in [16]. In [17], a stable potential field between the leader and the follower robots during the operation is proposed, whereas an artificial potential fields method is introduced in [18]. The potential vectors are virtually constructed with respect to the center of geometry of the robots, the length of the vectors are kept constant during the operation [19], where a drone is responsible for identifying the global coordinates of each robot in the system. In [20], the localization problem is searched with panoramic cameras located on each unicycle robot providing the visual inputs to the autonomous swarm system. For complex systems dealing with NP-Hard problems [21], group-based distributed auction algorithms have been proposed to solve the swarm autonomous task assignment problem. Another visible light positioning technique with the help of odometer is employed for multi-robot cooperative navigation problem in [22].

The success of the autonomous systems is related with the see-think-act cycle [23]. The sensing units of each agent in the system should work in coherence to provide precise inputs to the main controller. Since the vision-based sensing units offer low cost and rich information of the surrounding environment [24], [25], they are often preferred in multi-robot autonomous systems compared to the LIDAR sensing [26]. On the other hand, signal-based tracking systems are also useful for autonomous systems, where they are preferably deployed by unmanned aerial vehicles [27]. The use of visual inputs containing only images can be deficient when depth information is desired for maintaining the specified distance between the agents. The Kinect sensor, providing both colored image and depth information were commonly used in the literature [28]. The formation control is converted to a trajectory tracking problem in which each agent maintains the relative distance between each other using the information from the Kinect sensors. It is underlined in the literature that the switching leader mechanism prevents the failure of the system in case of a malfunction of the leader agent [28]. In [29], a localization method for the follower robots was introduced. If there is an autonomous multi-robot system with decentralized controllers, then the Kinect sensors are located on each agent in the decentralized systems. The Kinect's maximum viewing angle should be considered during the system dynamics. Blind spots, if any, needed to be determined in the design stage. On the other hand, in centralized controller architectures, a single Kinect sensor, or any other type of visual sensor, may be enough to monitor the instantaneous relative positions of the agents. This monitoring can also be provided by the GPS systems or by an aerial vehicle equipped with a camera as in [19]. Transient dynamics of the formation controller is studied in [30], where an optical capturing system is managed from a central unit rather than employing inter-vehicle communication devices for each robot. Due to the dynamic conditions of complex environments, the authors have developed a reconfigurable shape formation of multi-robot systems based on a virtual linkage approach [31].

Since object delivery systems are frequently used in intelligent logistics, a non-contact prehensile payload carrying design using permanent magnets based on a leader-follower formation control is introduced in this study for a multi robot team. Although the multi-robot formation problem has been intensely studied, there is little research in the literature that performs magnetic object transportation where they commonly focus on transporting the objects within the robot, or on the carrier robot. In [32], a combination of global and local path planning algorithms for object search and delivery in unstructured environments was proposed. A speed-switching controller is employed in the controller strategy to cope with inclined roads in the environment. Those systems need more energy compared to the systems pushing the payload and are deficient when they are exposed to heavier loads. Hence, the main concern of this study is to develop a novel object transportation mechanism using magnetically actuated non-contact units. The payload is located on a wheeled cart that has magnets on each wall. The permanent magnets are mounted on the autonomous robots that interact with these walls to satisfy the transportation. The leader agent is responsible for stabilizing the locomotion, whereas the follower agents are responsible for thrusting the payload carrier cart. Based on the study published in [19], we assigned the payload carrier cart as a virtual leader of the system. A line shape formation is designed by using two robots. The mathematical model of the system is derived considering the non-holonomic robots, and a leader-follower controller strategy is developed by modifying the controller presented in [19]. Since the aim is an improved energy consumption and load capacity, MATLAB simulations using the Turtlebot2 differential drive robots were carried out. The contributions of the proposed study apart from the previous literature are highlighted as below:

1. A new mechanism for a prehensile payload transportation using permanent magnets is proposed.

2. The formation control problem is tackled by considering special cases such as turning from the sharp edges. Sub-controller rules are applied to maintain the caging of the payload during the cornering action.

3. An error analysis of the selected formation controller algorithm is carried out so that the payload deviation from the predefined trajectory satisfies an acceptable region of

operation.

The non-contact behavior of the object transportation method proposed in this work provides sensitive manipulation of the payload compared with the method published in [6], where continuous impulse exerts to the payload during the operation. Since the payload is not located on the robots as in [32], our method suggests longer service life of the robots due to the lack of vertical stress applied by the payload.

The rest of the paper is organized as follows: a system overview is given in Section 2, followed by the basic dynamic equations and mathematical model of the system in Section 3. Basic points of the formation controller are presented in Section 4. Section 5 gives the simulation setup and case scenarios of the system containing the relevant outputs of the study. In Section 6, concluding research remarks are provided.

2. System Overview

The multi-robot system in this study is responsible for transporting the payload in a robust way. It is a non-contact transportation by using permanent magnets attached to the robots and the wheeled cart carrying the payload. The magnets are located peripherally on the robots and the cart. The minimum distance idea between the magnets is considered to prevent rotation on pitch axis. The unlike poles of the magnets on the cart and the docking robot is selected to provide a non-contact locomotion. The cornering to prevent collision on the trajectory needs to be handled carefully since the rotation of the robots concurrently can cause instabilities. Hence, the linear velocity of the robots set to be zero when the robots adjust their angular orientation due to the obstacle. The formation configuration is conserved regardless of going straight or cornering. The system does not permit translational and rotational motion at the same time.

One of the key design selections of multi-robot autonomous systems is to locate the visual sensors in the whole architecture. Local sensing units like in [24] are used in the multi-robot system, where the tracking control of the followers is achieved by bypassing the communication between the robots. The followers are equipped with sensing units to identify the position of the leader. On the other hand, a global sensing unit is also used in the multi-robot systems [19], where the visual sensing is performed by a drone that can view all of the robots from a general perspective. Visual identifiers such as coloured tags were used to make the drone recognize each robot easily.

In this study, a visual tag is intended to be placed on the payload carrier cart in the center point with a reasonable height with respect to the Kinect sensors mounted on the Turtlebot2 robots. The docking action of the robots to the cart is based on the visual information gathered by the Kinect sensors. The orientation of the leader robot is always in the same direction with the motion. Thus, when the leader robot approaches to the cart, it should make a 180° full turn before the cooperative motion. The follower robot does not need any extra turning as the docking and motion directions are the same for the follower robot. In Figure 1 the system overview is given.

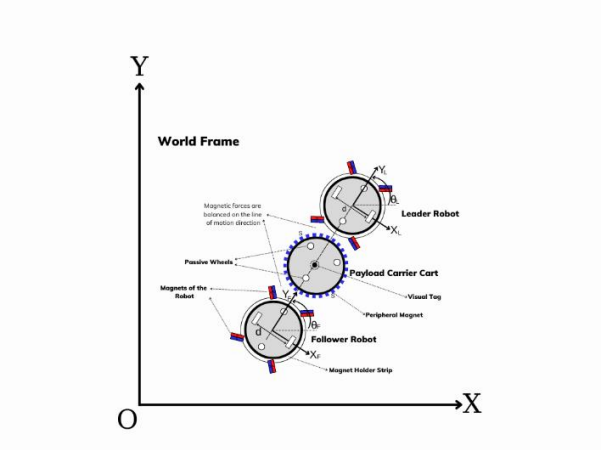

Figure 1. System Overview

A magnet supported transportation system with wheeled cart can cause vibrations in the system. Therefore, the vibration suppression problem with the disturbances are considered. The force balance in the system is maintained by the controller. The main concern of this study is to maintain a robust cooperative locomotion. To ensure this, three different action scenarios were studied. The first scenario is the search of the payload mounted on the wheeled cart executed by the robots. When the cart is detected, the robots are ready to go to the correct positions for the docking action. The second scenario is the docking action of the robots to the cart. The visual information helps the robots in this stage. The final action is the cooperative locomotion of the robots to transport the payload to the target delivery point.

3. Overall Structure

A Turtlebot2 equipped with a Kinect sensor providing an image information of the surrounding space in a specific angular range is used in this study. Since the Kinect sensor provides depth information of the recognized objects, it is preferred to maintain the distance between the leader and the follower. The Turtlebot has two differential wheels for locomotion and two caster wheels for stabilization. The distance between the active wheels is denoted by ‘d’ as shown in Figure 2.

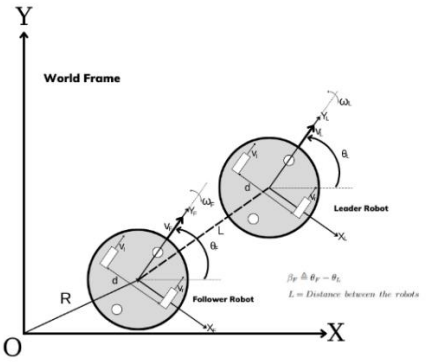

Figure 2. Coordinate System of the Leader and Follower Robots

When developing the mathematical model of the system, one robot is selected as the leader, whereas the other robots are selected as followers. Based on the selected configuration, the number of the followers can change. For a two robot system, a line formation is preferred with a single follower. Different formation styles are shown in Figure 3. The number of robots can be adjusted based on the size and weight of the payload. In this study, a line configuration with two robots is considered.

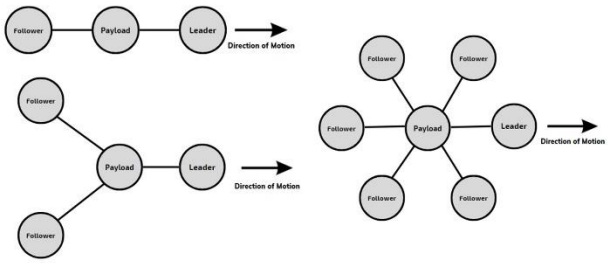

Figure 3. Selected Formation Styles

3.1. System Dynamics

The dynamics of the robot is presented by adopting the model presented in [9]. The motions of the robots were obtained from the linear and the angular velocities assuming no-slip condition.

The velocities of the active wheels determine the linear and angular velocities of the robot. The difference between the velocities of the active wheels creates rotational motion. The velocities of the left and right wheels are defined as in (1) and (2).

$$v_l = r\dot{\phi}_l \tag{1}$$

$$v_r = r\dot{\phi}_r \tag{2}$$

In (1) and (2), r denotes the radius of the wheels and $\dot{\phi}_r$ and $\dot{\phi}_l$ denote the angular velocities of the left and right wheels respectively.

By using (1) and (2), linear and angular velocities of the robot are calculated as in (3) and (4):

$$v = \frac{v_l + v_r}{2} = \frac{r(\dot{\phi}_l + \dot{\phi}_r)}{2} \tag{3}$$

$$\omega = \frac{v_l - v_r}{d} = \frac{r(\dot{\phi}_l - \dot{\phi}_r)}{d} \tag{4}$$

The direction of the angular velocity of the robot is determined by the comparison of the velocities of the left and right wheels. If the left active wheel's speed is higher than the right one, the robot will turn to right and vice versa. If the active wheel speeds are equal, then the robot will move forward.

The final state equation is obtained in (8) by using (5), (6), and (7):

$$\dot{x}_i = v\cos\theta_i \tag{5}$$

$$\dot{y}_i = v\sin\theta_i \tag{6}$$

$$\dot{\theta}_i = \omega \tag{7}$$

$$\begin{bmatrix}\dot{x}_L \\ \dot{y}_L \\ \dot{\theta}_L\end{bmatrix} = \begin{bmatrix}\cos\theta_L & 0 \\ \sin\theta_L & 0 \\ 0 & 1\end{bmatrix}\begin{bmatrix}v_L \\ \omega_L\end{bmatrix} \tag{8}$$

The control variables of the system are found to be the linear and angular velocities $[v_L, \omega_L]$ of the leader robot. Now we have to define the state equations of the follower robot with respect to the leader based on the model presented in [24].

The position of the follower robot with respect to the leader can be expressed in the following form:

$$\boldsymbol{r}_F = R(-\theta_F)(\boldsymbol{r}_F - \boldsymbol{r}_L) \tag{9}$$

The time derivative of the position vector is taken to obtain the velocity vector as below:

$$\dot{\boldsymbol{r}}_F = \dot{\boldsymbol{R}}(-\theta_L)(\boldsymbol{r}_F - \boldsymbol{r}_L) + R(-\theta_L)(\dot{\boldsymbol{r}}_F - \dot{\boldsymbol{r}}_L) \tag{10}$$

In (10), the rotation matrix of the leader with respect to the world frame is defined as below:

$$\boldsymbol{R}(-\theta_L) = \begin{bmatrix}\cos\theta_L & \sin\theta_L \\ -\sin\theta_L & \cos\theta_L\end{bmatrix} \tag{11}$$

The time derivative of the rotation matrix is given below:

$$\dot{\boldsymbol{R}}(\theta_L) = \begin{bmatrix} 0 & \omega_L \\ -\omega_L & 0 \end{bmatrix} \boldsymbol{R}(-\theta_L) \tag{12}$$

The previous equations are replaced with their equivalents in the velocity expression of the follower as below:

$$\begin{bmatrix} \dot{x}_F \\ \dot{y}_F \end{bmatrix} = \begin{bmatrix} -1 & y_F \\ 0 & -x_F \end{bmatrix} \begin{bmatrix} v_L \\ \omega_L \end{bmatrix} + \begin{bmatrix} \cos(\theta_F - \theta_L) \\ \sin(\theta_F - \theta_L) \end{bmatrix} v_F \tag{13}$$

At this point, a new variable as the angular difference between the follower and the leader is defined. Based on the system architecture developed in this study, angular difference between the robots plays a key role to maintain the stability of the cooperative locomotion. The controller adjusts this difference based on the formation configuration.

$$\beta_F = \theta_F - \theta_L \tag{14}$$

The time derivative of the angular difference variable is given below.

$$\dot{\beta}_F = \omega_F - \omega_L \tag{15}$$

We reorganized the system dynamics equation by embedding the angular difference variable into the relevant equations.

$$\begin{bmatrix} \dot{x}_F \\ \dot{y}_F \\ \dot{\beta}_F \end{bmatrix} = \begin{bmatrix} \cos\beta_F & 0 \\ \sin\beta_F & 0 \\ 0 & 1 \end{bmatrix} \boldsymbol{u}_F + \begin{bmatrix} -1 & y_F \\ 0 & -x_F \\ 0 & -1 \end{bmatrix} \boldsymbol{u}_L \tag{16}$$

The control variables of the follower and the leader are given as $u_F = [v_F \quad \omega_F]$ and $u_L = [v_L \quad \omega_L]$ in (16).

Now that we have reached a general systems dynamics equation for a multi robot system consists of one leader and one follower robots. This system of equations can be further expanded for high number of leaders and followers by defining the state equations of each robot in the system.

The linear and angular velocities of the robots are limited by the properties of the Turtlebot2 robotic platform.

3.2. Formation Model

During the locomotion of the robots with the payload, the controller tries to minimize the error between the actual and desired positions of the states. The displacements between the leader and the follower robots are defined as below:

$$\begin{bmatrix} x_F^d \\ y_F^d \\ \beta_F^d \end{bmatrix} = \begin{bmatrix} L_{xF} \\ L_{yF} \\ 0 \end{bmatrix} \tag{17}$$

For any configuration, the formation geometry is conserved by the controller at each time step of the motion.

The error rates are given below.

$$\begin{bmatrix} \epsilon_{xF} \\ \epsilon_{yF} \end{bmatrix} = \begin{bmatrix} x_F - L_{xF} \\ y_F - L_{yF} \end{bmatrix} \tag{18}$$

The leader robot is always within the follower's field of vision. The angle of view of the Kinect gives greater values than the angular difference oscillating around zero.

4. Formation Controller

The formation control algorithm in [19] is used in this study where the potential functions between the leader and the follower robots are introduced. This control algorithm is proven to have a light computation burden and an ease of implementing to the actual robots. Concerning these advantages, this algorithm is preferred in this study. The location of the payload carrier cart is selected as the center of the multi robot system where the controller tries to keep the desired distances between the agents and the center in an acceptable error. The virtual leader is the payload carrier cart where each robot should adjust its position with respect to the virtual leader. In this method, there is a single reference point, which simplifies the controller algorithm. The potential functions are calculated both between the center and the robots and within the robots. In Figure 4, potential functions are shown in a line formation. The linear and angular velocities of the virtual leader are bounded.

The sole mission of the controller is to decide on the position of the virtual leader. During the cooperative motion of the robots transporting the payload, each robot should maintain the desired potential functions.

The position of the virtual leader is defined as:

$$x_{VL} = \frac{x_L + x_F}{2} \tag{19}$$

$$y_{VL} = \frac{y_L + y_F}{2} \tag{20}$$

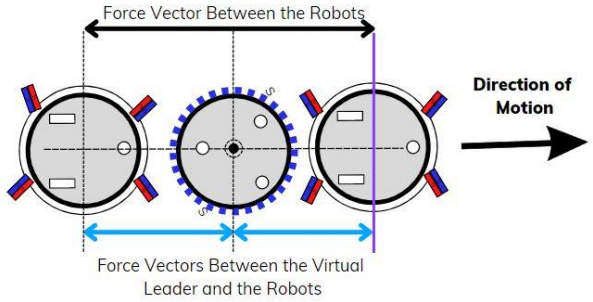

Figure 4. Potential Function of the Formation Controller

where, x_{VL} and y_{VL} denote the coordinates of the virtual leader, whereas x_L, y_L, x_F, y_F denote the coordinates of the leader and the follower robots respectively.

The potential functions between the virtual leader and the robots are defined as:

$$P_{xL}^{VL} = K\Delta d_{XL}^{VL} \quad (21)$$

$$P_{xF}^{VL} = K\Delta d_{XF}^{VL} \quad (22)$$

$$P_{yL}^{VL} = K\Delta d_{yL}^{VL} \quad (23)$$

$$P_{yF}^{VL} = K\Delta d_{yF}^{VL} \quad (24)$$

Here, P_{xL}^{VL}, P_{xF}^{VL}, P_{yL}^{VL}, and P_{yF}^{VL} denote the potential functions of the robots with respect to the virtual leader. K is the gain of the function that is adjusted by the controller. $\Delta d_{XL}^{VL}, \Delta d_{XF}^{VL}, \Delta d_{yL}^{VL}, \Delta d_{yF}^{VL}$ denote the distance difference between the current position and the initial position.

$$d_{XL}^{VL} = (x_{VL} - x_L) - (x_{VL0} - x_{L0}) \quad (25)$$

$$d_{XF}^{VL} = (x_{VL} - x_F) - (x_{VL0} - x_{F0}) \quad (26)$$

$$d_{yL}^{VL} = (y_{VL} - y_L) - (y_{VL0} - y_{L0}) \quad (27)$$

$$d_{yF}^{VL} = (y_{VL} - y_F) - (y_{VL0} - y_{F0}) \quad (28)$$

The potential functions between the leader and the follower robots are defined as:

$$P_X^{LF} = K_{LF}\Delta d_X^{LF} \quad (29)$$

$$P_y^{LF} = K_{LF}\Delta d_y^{LF} \quad (30)$$

The potential function between the agents is reversible. K_{LF} is the gain of the function. Random disturbances are added to the system to represent the oscillations of the robots arising during magnetic docking. The position differences are defined as:

$$\Delta d_X^{LF} = (x_{LF} - x_L) - (x_{LF0} - x_{L0}) \quad (31)$$

$$\Delta d_y^{LF} = (y_{LF} - y_L) - (y_{LF0} - y_{L0}) \quad (32)$$

The controller is responsible for keeping the distances and the angular difference between the leader and the follower robots in an acceptable error. The potential functions complement each other in the sense of selected formation.

5. Simulations

Three different scenarios are investigated in this section. The first scenario searches for the robot's docking capabilities through the payload. Secondly, turning from sharp corners is simulated. The third scenario is about the transportation of the payload through a predefined trajectory. All of the simulations were conducted via MATLAB with a group of two non-holonomic differential drive robots transporting a payload carrier cart with passive wheels in a line formation.

5.1. Docking to the Payload

In this scenario, the main concern is to transport the payload to the target area in a robust way. A* searching algorithm was used to transport payload carrier wheeled cart [33]. The algorithm is updated based on the environment and conditions of this study. Generic simulations for the leader and the follower robots in a line formation configuration are conducted. Optimal trajectories are shown for different starting points of the robots in Figure 5.

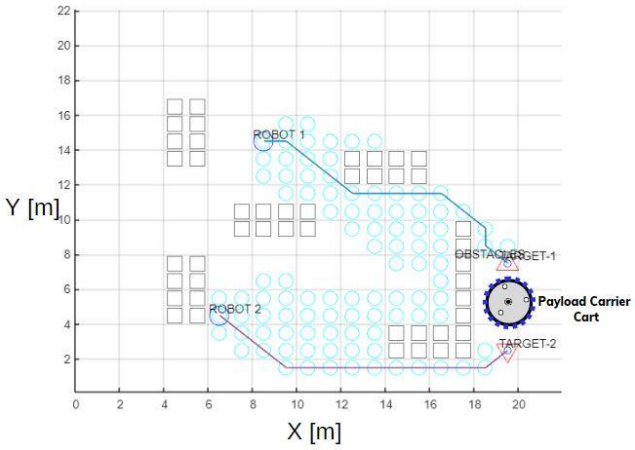

Figure 5. Optimal Trajectories Reached in Object Search Simulation Results

5.2. Cornering Action

The payload is carried by a circular cart with passive wheels. There are permanent magnets installed on this cart interacting with other permanent magnets installed on the robots in such a way that the controller supplies stable motion with slight oscillations. However, a failure can be observed during cornering on the predefined trajectory. The non-contact mechanism might deviate from its desired operation point due to the torque effects of magnetic forces while cornering. Therefore, a special sub-controller for controller is developed. The leader and follower robots adjust their orientation before the cornering action to resume stable propulsion of the payload. Figures 6, 7, and 8 show the basic points of the cornering step by step. The leader robot adjusts its orientation by turning around itself, while the follower robot changes both its orientation and position to sustain magnetic docking of the payload carrier cart without failures.

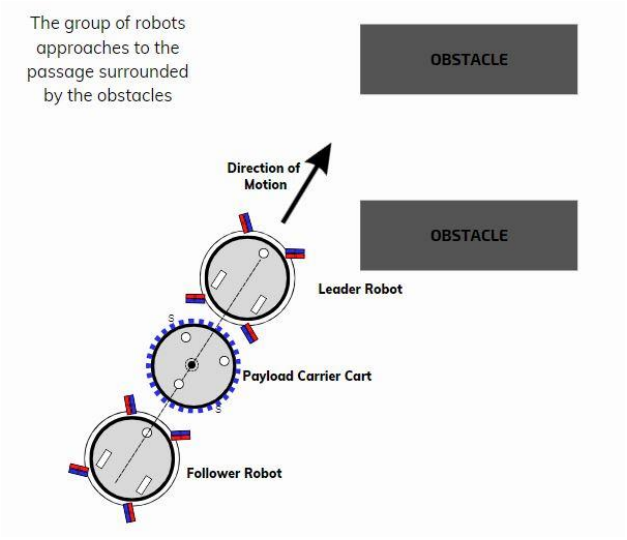

Figure 6. Robots approaching to the cornering point

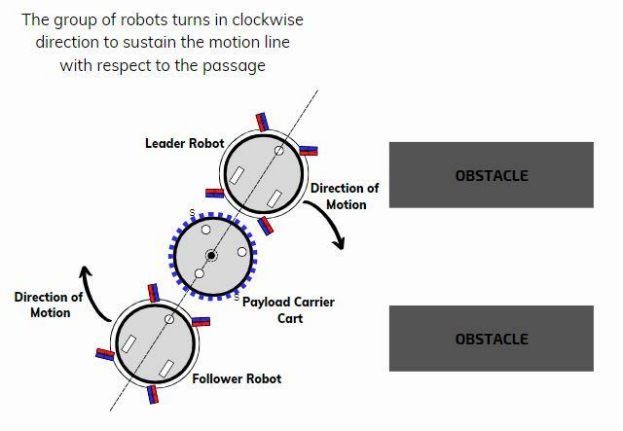

Figure 7. Robots adjust their orientation before passing through the corridor

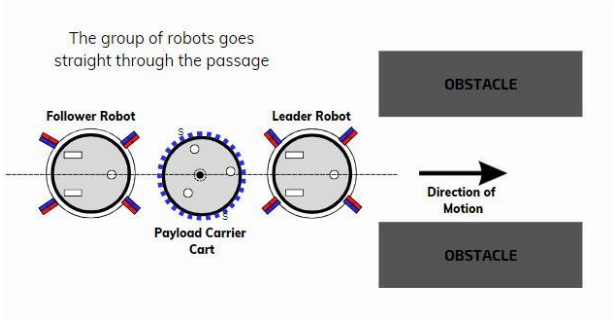

Figure 8. Robots continue on their trajectory

The controller tries to avoid continuous motion while passing through sharp corners for a stable operation. A generic simulation for cornering using the developed controller is conducted via MATLAB Robotic Toolbox. The resulting motion is shown in Figure 9.

5.3. Transportation of the Payload

For payload transportation, an ellipsoid trajectory without obstacles and an obstacle-based trajectory like a labyrinth are taken into consideration. In the first case, the payload is transported in a predefined generic ellipsoid trajectory without obstacles. The mean errors for varying controller gain values are evaluated to show the reliability of the controller. Figure 10 shows the simulation results. It is seen that the trajectory is successfully followed.

It is found out that the minimum error rates are obtained in k = [0.75 1.00] range, whereas the stability cannot be preserved for the gain values higher than 2. A detailed view of robot's motion is shown in Figure 11.

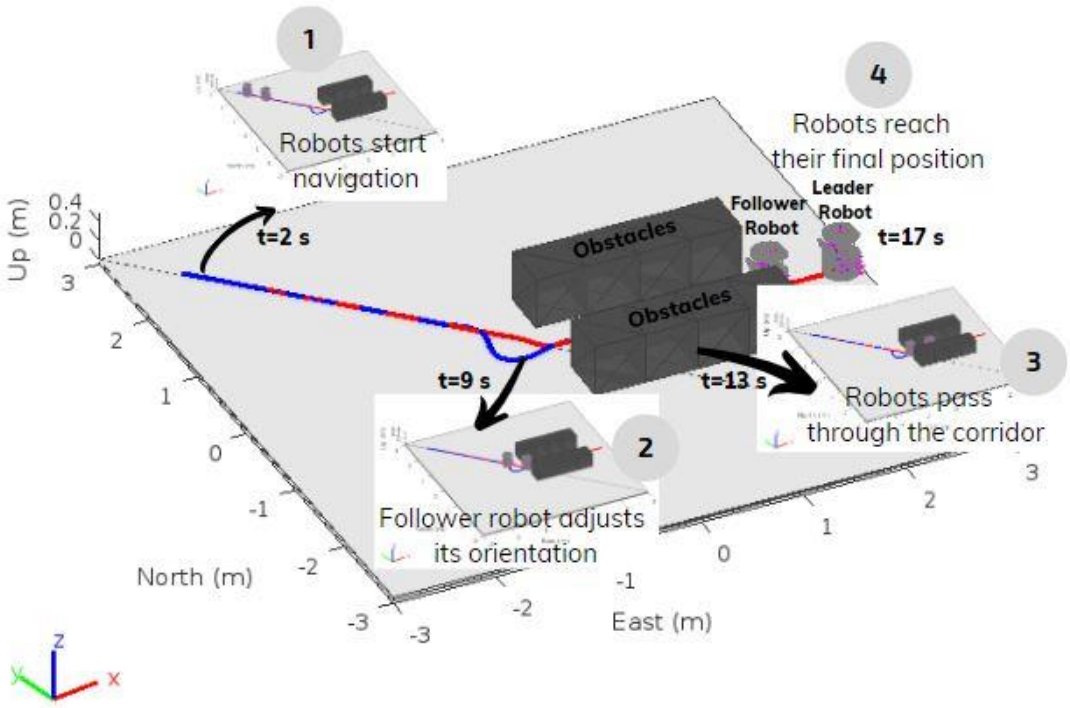

Figure 9. Simulation Result of the Cornering

An environment model with obstacles is introduced in the second scenario. We have built up an environment with box shaped walls like obstacles which can be also realized with actual Turtlebot2 experiments. Both the 2D and 3D views of the environment are shown in Figure 12.

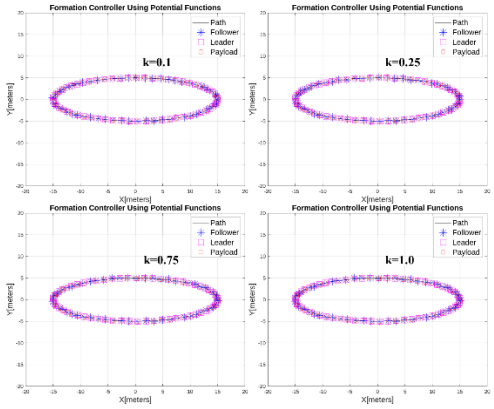

Figure 10. Ellipsoid Trajectory Simulations

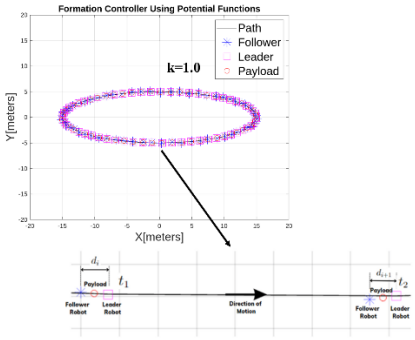

Figure 11. Path of the follower robot

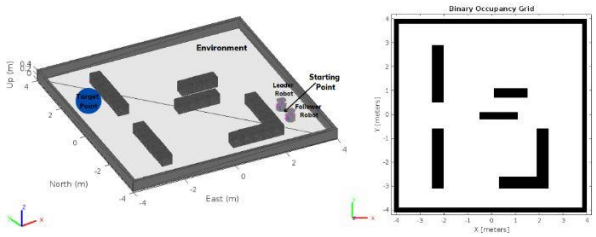

Figure 12. Simulation Environment

Two Turtlebot2 robot models are loaded into our environment. The start and the target points are specified. The starting point is specified with respect to the position of the payload. The starting positions of the leader and follower robot are q1 = [3 −1.5 0] and q2 = [3 −2.25 0] respectively. The simulation is conducted based on an optimum trajectory between the start and end points determined by the developed controller algorithm. The simulation results are shown in Figure 13. The controller updates potential functions introduced in Section IV at each time step to keep the virtual leader at the desired location. The linear and angular velocity commands for both the leader and follower robots are computed with respect to the desired potential functions.

Based on the simulation results, the position of the virtual leader is shown in Figure 14.

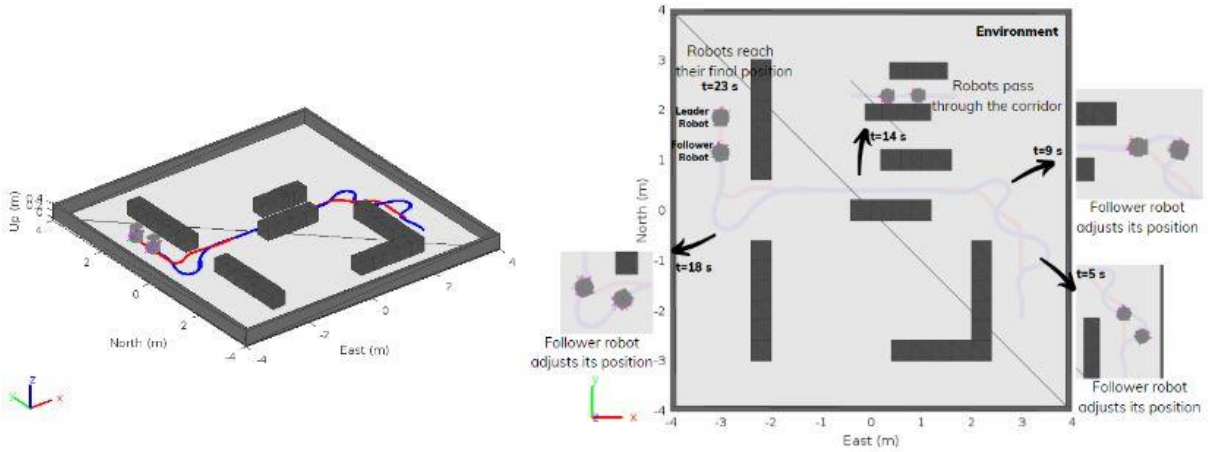

Figure 13. Simulation Result in the Environment

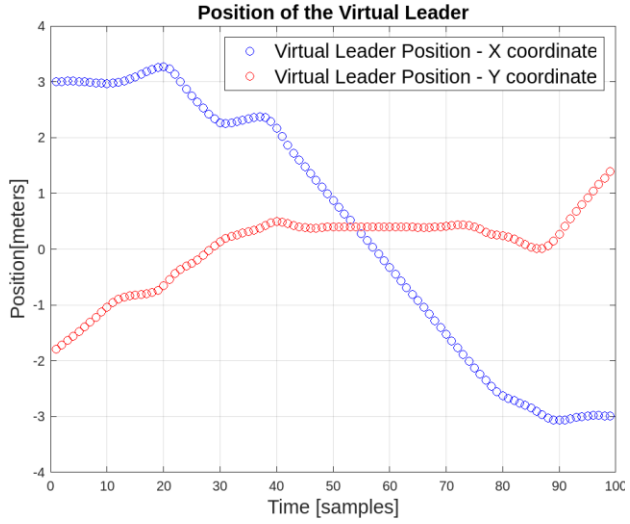

Figure 14. Position of the Virtual Leader

The formation controller's goal is to maintain a fixed distance value in the desired range. When the leader robot decides to change its direction with respect to a cornering point, the follower reacts by changing its orientation to keep the virtual leader, i.e. the payload carrier cart, at the center of geometry point. The deviations of the follower path from the optimum trajectory are due to this reaction. Three cornering points and the resulting three deviations are shown in Figure 13. While the follower robot is adjusting its orientation to keep the payload in the center of geometry, the leader robot waits for the formation to be ready to keep going on the trajectory.

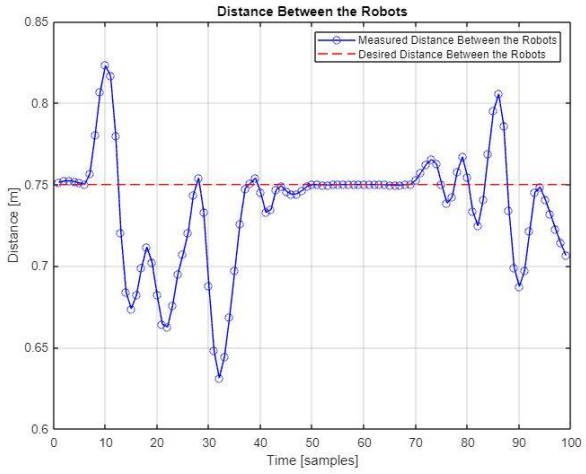

Figure 15. Distance Between the Robots

Figure 15 and Figure 16 show the distance between the robots and angular differences between the robots respectively. Since the follower robot adjusts its orientation before cornering, deviations from the desired value of distance and angular difference are observed.

When errors in distance values are evaluated, it is seen that the system is in the acceptable range of error. The angular difference values have exceeded 30◦, because the orientation of the follower robot will take some time to recover the leader's trajectory.

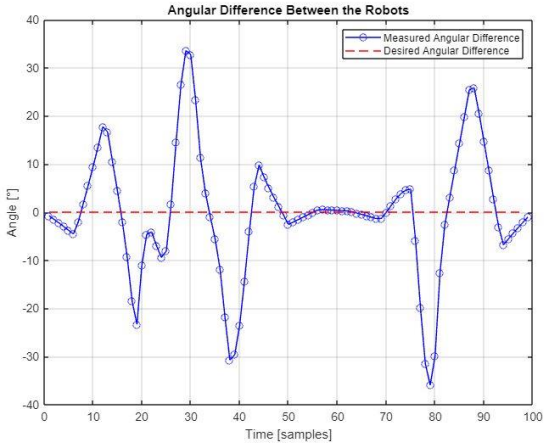

Figure 16. Angular Difference Between the Robots

To evaluate the performance of the controller, a time window including the straight line motion from the simulation is selected as t(straight) = [50 65]. The reason for splitting the simulation is that the robots have a combined motion of straight line navigation and cornering. The distance errors between the robots for the straight line motion are illustrated in Figure 17. The desired distance is 0.75 m. The root mean square errors for distance and angle are calculated as 1.46×10^{-4} [m] and 0.99 [◦].

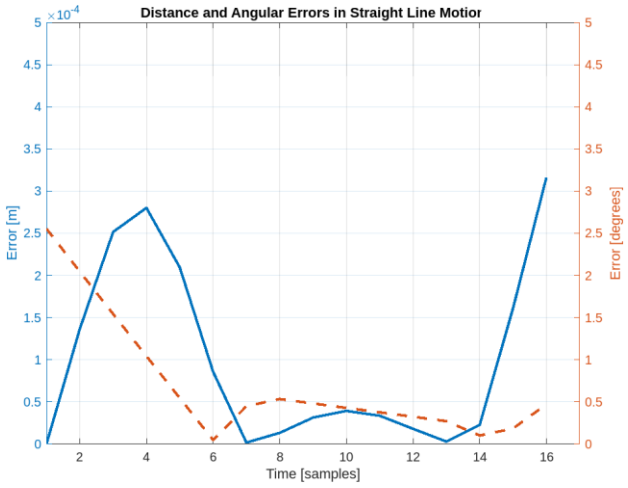

Figure 17. Distance and Angular Errors in Straight Line Motion

Another time window including a cornering from the simulation is selected as t(cornering) = [10 40]. The error values between the robots for the specified cornering are illustrated in Figure 18. The root mean square errors for distance and angle are calculated as 0.0605 [m] and 17.18 [◦] respectively.

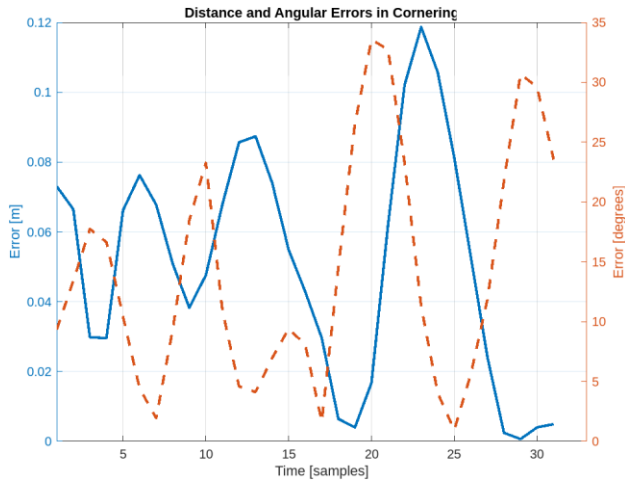

Figure 18. Distance and Angular Errors in Cornering

Moreover, a robustness metric including the distance and angular difference between the robots is introduced. Based on the physical design selections of the non-contact prehensile object transportation system, the penalty function is defined as below:

$$(d_1 \geq 0.45[m] \;||\; d_2 \geq 0.45[m]) \;\&\&\; |\beta| \geq 45[°] \qquad (33)$$

Here, d_1 and d_2 denote the distance between the leader robot and the payload and the follower robot and the payload respectively, whereas β denotes the angular difference between the leader and the follower robots. If the failure conditions occur as defined in (33), the payload carrier cart escapes from the caging of the leader and follower robots. This undesirable action aborts the operation and it starts from scratch with the first process of docking. The deviations of the distance values d_1 and d_2 of the simulation are shown in Figure 19.

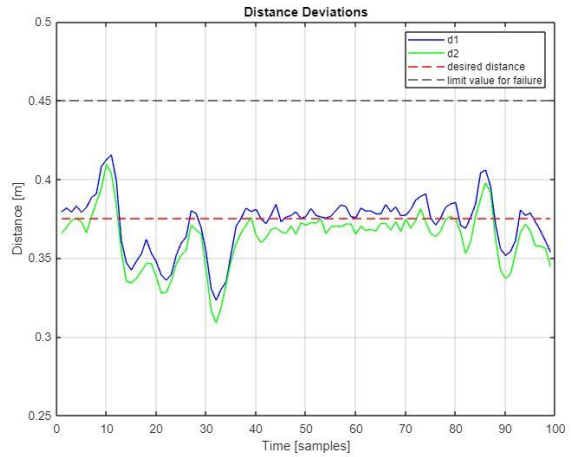

Figure 19. Distance Deviations

As it is seen from Figure 16 and Figure 19, the deviations and angular errors do not exceed the failure regions defined in (33), performing a stable ride. The results of the simulation verify our system for further stages of the research. The results obtained in this work are consistent with the study published in [19], in the sense of implementing an effective formation control method of multiple robots for a specific task. The error values are supported by the study published in [24] based on the visibility constraints. The path following capability reached in this work is compatible with the study published in [20].

6. Conclusions

In this study, a formation controller based on potential functions is developed for a novel object delivery system. The proposed system is based on propelling the payload with permanent magnets. Therefore, a non-contact transportation that offers an efficient way of object delivery is sustained. Our controller is verified for various simulation scenarios. The formation controller is a proven lightweight method for the multi-robot navigation and it is a proper way of controlling the robots in this study. The results of this paper are promising for actual experiments that are planned as a future study. Finally, it is envisioned that vision-based robotic solutions offer opportunities to design and implement intelligent object delivery systems.

Acknowledgment

This work was supported by Office of Scientific Research Projects of Karadeniz Technical University. Project number: FHD-2022-10233

The first author was partly supported by The Scientific and Technological Research Council of Türkiye under the Programme 2211-A.

References

[1] Coucerio, M. S., Portugal, D., Ferreira, J. F., Rocha, R.P., "Semfire: Towards a new generation of forestry maintenance multi-robot systems," in *2019 IEEE/SICE International Symposium on System Integration (SII)*, Paris, France, 2019, pp. 270-276, DOI: https://doi.org/10.1109/SII.2019.8700403

[2] Kronmueller, M., Fielbaum, A., Alonso-Mora, J., "On-demand grocery delivery from multiple local stores with autonomous robots," in *2021 International Symposium on Multi-Robot and Multi-Agent Systems (MRS)*, Cambridge, United Kingdom, 2021, pp. 29-37, DOI: https://doi.org/10.1109/MRS50823.2021.9620599

[3] Edlerman, E., Linker, R., "Autonomous multi-robot system for use in vineyards and orchards," in 2019 27th Mediterranean Conference on Control and Automation (MED), Akko, Israel, 2019, pp. 274-279, DOI: https://doi.org/10.1109/MED.2019.8798538

[4] Moser, J., Hoffman, J., Hildebrand, R., Komendera, E., "An autonomous task assignment paradigm for autonomous robotic in-space assembly," *Frontiers in Robotics and AI*, vol. 9, February 2022, DOI: https://doi.org/10.3389/frobt.2022.709905

[5] Chen, Z., Emami, M.R., Chen, W., "Connectivity preservation and obstacle avoidance in small multi-spacecraft formation with distributed adaptive tracking control," *Journal of Intelligent & Robotic Systems*, vol. 101, article no. 16, December 2020, DOI: https://doi.org/10.1007/s10846-020-01269-y

[6] Wan, W., Shi, B., Wang, Z., Fukui, R., "Multirobot object transport via robust caging," *IEEE Transactions on Systems,*

Man, and Cybernetics: Systems, vol. 50, issue 1, pp. 270-280, August 2017, DOI: https://doi.org/10.1109/TSMC.2017.2733552

[7] Consolini, L., Morbidi, F., Prattichizzo, D., Tosques, M., "Leader–follower formation control of nonholonomic mobile robots with input constraints," *Automatica*, vol. 44, issue 5, pp. 1343-1349, May 2008, DOI: https://doi.org/10.1016/j.automatica.2007.09.019

[8] Moorthy, S., Joo, Y.H., "Formation control and tracking of mobile robots using distributed estimators and a biologically inspired approach," *Journal of Electrical Engineering & Technology*, August 2022, DOI: https://doi.org/10.1007/s42835-022-01213-0

[9] Das, A.K., Fierro, R., Kumar, V., Ostrowski, J.P., Spletzer, J., Taylor, C.J., "A vision-based formation control framework," *IEEE Transactions on Robotics and Automation*, vol. 18, issue 5, pp. 813-825, October 2002, DOI: https://doi.org/10.1109/TRA.2002.803463

[10] Xiao, H., Li, Z., Philip Chen, C.L., "Formation control of leader–follower mobile robots' systems using model predictive control based on neuraldynamic optimization," *IEEE Transactions on Industrial Electronics*, vol. 63, issue 9, pp. 5752-5762, March 2016, DOI: https://doi.org/10.1109/TIE.2016.2542788

[11] Recker, T., Heinrich, M., Raatz, A., "A comparison of different approaches for formation control of nonholonomic mobile robots regarding object transport," in Procedia CIRP 2021, vol. 96, pp. 248-253 DOI: https://doi.org/10.1016/j.procir.2021.01.082

[12] Freda, L., Gianni, M., Pirri, F., Gawel, A., Dube, R., Siegwart, R., Cadena, C., "3d multi-robot patrolling with a two-level coordination," *Autonomous Robots*, vol. 43, issue 7, pp. 1747-1779, October 2019, DOI: https://doi.org/10.1007/s10514-018-09822-3

[13] Miao, Z., Liu, Y.-H., Wang, Y., Yi, G., Fierro, R., "Distributed estimation and control for leader-following formations of nonholonomic mobile robots," *IEEE Transactions on Automation Science and Engineering*, vol. 15, issue 4, pp. 1946-1954, March 2018, DOI: https://doi.org/10.1109/TASE.2018.2810253

[14] Wang, B., Wang, J., Zhang, B., Chen, W., Zhang, Z., "Leader–follower consensus of multivehicle wirelessly networked uncertain systems subject to nonlinear dynamics and actuator fault," *IEEE Transactions on Automation Science and Engineering*, vol. 15, issue 2, pp. 492-505, January 2017, DOI: https://doi.org/10.1109/TASE.2016.2635979

[15] Lashkari, N., Biglarbegian, M., Yang, S.X., "Development of a novel robust control method for formation of heterogeneous multiple mobile robots with autonomous docking capability," *IEEE Transactions on Automation Science and Engineering*, vol. 17, issue 4, pp. 1759-1776, April 2020, DOI: https://doi.org/10.1109/TASE.2020.2977465

[16] Yan, B., Shi, P., Lim, C.-C., "Robust formation control for nonlinear heterogeneous multiagent systems based on adaptive event-triggered strategy," *IEEE Transactions on Automation Science and Engineering*, vol. 19, issue 4, pp. 2788-2800, October 2022, DOI: https://doi.org/10.1109/TASE.2021.3103877

[17] Elkaim, G.H., Kelbley, R.J., "A lightweight formation control methodology for a swarm of non-holonomic vehicles," in *2006 IEEE Aerospace Conference 2006, Big Sky, MT, USA, March 4-11, 2006*, IEEE, 2006. pp. 8.-, DOI: https://doi.org/10.1109/AERO.2006.1655803

[18] Harder, S.A., Lauderbaugh, L.K., "Formation specification for control of active agents using artificial potential fields," *Journal of Intelligent & Robotic Systems*, vol. 95, issue 2, pp. 279-290, August 2018, DOI: https://doi.org/ https://doi.org/10.1007/s10846-018-0912-7

[19] Gallardo, N., Pai, K., Erol, B.A., Benavidez, P., Jamshidi, M., "Formation control implementation using kobuki turtlebots and parrot bebop drone," in *2016 World Automation Congress (WAC) 2016, Rio Grande, PR, USA, July 31 – August 04, 2016*, IEEE, 2016. pp. 1-6, DOI: https://doi.org/10.1109/WAC.2016.7582996

[20] Mariottini, G.L., Morbidi, F., Prattichizzo, D., Vander Valk, N., Michael, N., Pappas, G., Daniilidis, K., "Vision-based localization for leader–follower formation control," *IEEE Transactions on Robotics*, vol. 25, issue 6, pp. 1431-1438, December 2009, DOI: https://doi.org/10.1109/TRO.2009.2032975

[21] Bai, X., Fielbaum, A., Kronmuller, M., Knoedler, L., Alonso-Mora, J., "Group-based distributed auction algorithms for multi-robot task assignment," *IEEE Transactions on Automation Science and Engineering*, Early Access, pp. 1-12, May 2022, DOI: https://doi.org/10.1109/TASE.2022.3175040

[22] Yan, Z., Guan, W., Wen, S., Huang, L., Song, H., "Multirobot cooperative localization based on visible light positioning and odometer," *IEEE Transactions on Instrumentation and Measurement*, vol. 70, article no: 7004808, June 2021, DOI: https://doi.org/10.1109/TIM.2021.3086887

[23] Siegwart, R., Nourbakhsh, I.R., Scaramuzza, D., Introduction to Autonomous Mobile Robots. Cambridge, Massachusetts, USA: MIT Press, 2011.

[24] Liu, X., Ge, S.S., Goh, C.-H., "Vision-based leader–follower formation control of multiagents with visibility constraints," *IEEE Transactions on Control Systems Technology*, vol. 27, issue 3, pp. 1326-1333, May 2019, DOI: https://doi.org/10.1109/TCST.2018.2790966

[25] Fallah, M.M.H., Janabi-Sharifi, F., Sajjadi, S., Mehrandezh, M., "A visual predictive control framework for robust and constrained multi-agent formation control," *Journal of Intelligent & Robotic Systems*, vol. 105, issue 4, article no: 72, July 2022, DOI: https://doi.org/10.1007/s10846-022-01674-5

[26] Das Sharma, K., Chatterjee, A., Rakshit, A., "A pso–lyapunov hybrid stable adaptive fuzzy tracking control approach for vision-based robot navigation," *IEEE Transactions on Instrumentation and Measurement*, vol. 61, issue 7, pp. 1908-1914, July 2012, DOI: https://doi.org/10.1109/TIM.2012.2182868

[27] Doostmohammadian, M., Taghieh, A., Zarrabi, H., "Distributed estimation approach for tracking a mobile target via formation of uavs," *IEEE Transactions on Automation Science and Engineering*, vol. 19, issue 4, pp. 3765-3776, October 2022, DOI: https://doi.org/10.1109/TASE.2021.3135834

[28] Besseghieur, K.L., Trebinski, R., Kaczmarek, W., Panasiuk, J., "Leaderfollower formation control for a group of ros-enabled mobile robots," in *2019 6th International Conference on Control, Decision and Information Technologies (CoDIT) 2019, Paris, France, April 23-26, 2019*, IEEE, 2019, pp. 1556-1561. DOI: https://doi.org/10.1109/CoDIT.2019.8820460

[29] Li, R., Li, Y., "Localization of leader-follower formations using kinect and rtk-gps," in *2014 IEEE International Conference on Robotics and Biomimetics (ROBIO 2014), Bali, Indonesia, December 5-10, 2014*, IEEE, 2014, pp. 908-913. DOI: https://doi.org/10.1109/ROBIO.2014.7090448

[30] Zhang, J., Shao, X., Zhang, W., Na, J., "Path-following control capable of reinforcing transient performances for networked mobile robots over a single curve," *IEEE Transactions on Instrumentation and Measurement*, Early Access, pp. 1-1, September 2022, DOI: https://doi.org/10.1109/TIM.2022.3201930

[31] Liu, Y., Gao, J., Liu, C., Zhao, F., Zhao, J., "Reconfigurable formation control of multi-agents using virtual linkage approach," *Applied Sciences*, vol. 8, issue 7, article no: 1109, July 2018, DOI: https://doi.org/10.3390/app8071109

[32] Gao, K., Xin, J., Cheng, H., Liu, D., Li, J., "Multi-mobile robot autonomous navigation system for intelligent logistics," in 2018 Chinese Automation Congress (CAC 2018), Xi'an, China, November 30 – December 02, 2018, IEEE, 2018, pp. 2603-2609. DOI: https://doi.org/10.1109/CAC.2018.8623343

[33] Varol, O.F., "Control based heuristic motion planning in cooperative mobile robots," M.S. thesis, Dept. of Control and Automation Eng., Yıldız Technical Univ., İstanbul, Türkiye, 2009.